The EMBO Journal (2006) 25, 1720–1729 | © 2006 European Molecular Biology Organization | All Rights Reserved 0261-4189/06
www.embojournal.org

THE EMBO JOURNAL

Glycine–alanine repeats impair proper substrate unfolding by the proteasome

Martin A Hoyt[1,3], Judith Zich[1,3], Junko Takeuchi[1], Mingsheng Zhang[1], Cedric Govaerts[2] and Philip Coffino[1,*]

[1]Department of Microbiology and Immunology, University of California, San Francisco, CA, USA and [2]Department of Cellular and Molecular Pharmacology, University of California, San Francisco, CA, USA

Proteasome ATPases unravel folded proteins. Introducing a sequence containing only glycine and alanine residues (GAr) into substrates can impair their digestion. We previously proposed that a GAr interferes with the unfolding capacity of the proteasome, leading to partial degradation of products. Here we tested that idea in several ways. Stabilizing or destabilizing a folded domain within substrate proteins changed GAr-mediated intermediate production in the way predicted by the model. A downstream folded domain determined the sites of terminal proteolysis. The spacing between a GAr and a folded domain was critical for intermediate production. Intermediates containing a GAr did not remain associated with proteasomes, excluding models whereby retained GAr-containing proteins halt further processing. The following model is supported: a GAr positioned within the ATPase ring reduces the efficiency of coupling between nucleotide hydrolysis and work performed on the substrate. If this impairment takes place when unfolding must be initiated, insertion pauses and proteolysis is limited to the portion of the substrate that has already entered the catalytic chamber of the proteasome.

The EMBO Journal (2006) **25,** 1720–1729. doi:10.1038/sj.emboj.7601058; Published online 6 April 2006
Subject Categories: proteins
Keywords: ATPase; Gly–Ala repeat; proteasome; protein structure; protein unfolding

Introduction

Proteasomes are the major neutral protease of eukaryotic cells. They constitute the effector arm of the ubiquitin–proteasome system, which first tags proteins, usually by ubiquitin chain conjugation, and then delivers them to the proteasome, where they are cleaved to peptides. Proteasomes are ATP-dependent proteases. A feature common to these taxonomically and structurally diverse molecular machines is the sequestration of proteolytic sites within a closed chamber (Pickart and Cohen, 2004). Substrate specificity is conferred by the ubiquitin tagging system, which licenses proteins to enter the chamber. Within that closed space, destruction is relatively independent of substrate sequence. Access is through a narrow pore (<15 Å) positioned axially at either end of the barrel-shaped chamber (Lowe *et al*, 1995; Groll *et al*, 1997). Entry thus demands tag recognition, unfolding and insertion. Unfolding is essential, as folded proteins are too bulky to traverse the entryway.

Significant progress has been made in understanding substrate recognition and proteolysis, but the intermediate processes of unfolding and insertion have substantially eluded investigation. The proteasome consists of the proteolytic 20S core particle capped at one end or at both ends by the 19S regulatory complex. This complex includes at least 18 distinct proteins, of which six are ATPases (Glickman *et al*, 1998). In eukaryotes, each ATPase is distinct; all are essential (Rubin *et al*, 1998). Hexameric ATPase rings, members of the very diverse AAA ATPase family, have the general capacity to change the conformation of their substrates (Vale, 2000), fueled by a cycle of ATP binding, hydrolysis and release. These general considerations imply that the ATPases of the proteasome are the key mediators of substrate unfolding and insertion, an inference with experimental support (Liu *et al*, 2002b). The hexameric ClpX ATPase of the ClpXP protease, an architecturally similar but distantly related ATP-dependent protease of bacteria, has been shown to utilize ATP when degrading a fully unfolded protein and to consume substantially more ATP if the same protein is presented in a folded form (Kenniston *et al*, 2003). Experiments of this kind have demonstrated that the energy cost of selective protein destruction is similar in magnitude to that used for protein translation. How ATP-sourced energy is produced and consumed within the proteasome is therefore important both for understanding its function and in evaluating the overall energy budget of the cell.

One way to understand the capacity and limits of a system of energy production and use is to challenge it with loads that drive it to failure. This is not easy to do with proteasomes. They are a general-purpose protein disposal machine and must be engineered, perhaps over-engineered, to deal with substrates of very diverse structure. One substrate that causes them to fail is the EBNA1 protein of Epstein–Barr virus (Levitskaya *et al*, 1995; Levitskaya *et al*, 1997). It contains an amino-acid tract consisting entirely of glycine and alanine residues, termed the glycine–alanine repeat (GAr). This varies from about 60 to 300 residues in different viral isolates. The GAr acts in *cis* to impair EBNA1 degradation by the proteasome; the GAr is also *cis*-inhibitory when transferred to various other proteins. Our laboratory recently showed that a GAr does not prevent substrate recognition by the proteasome, or impair initiation of degradation, but instead causes degradation to stall, rather than go to completion (Zhang and Coffino, 2004). Stalling can result in the production of partially processed intermediates that are trimmed at the end of the protein that first enters the proteasome (Zhang *et al*,

*Corresponding author. Department of Microbiology and Immunology, UCSF, 513 Parnassus Avenue, San Francisco, CA 94143-0414, USA. Tel.: +1 415 476 1783; E-mail: Philip.Coffino@ucsf.edu
[3]These authors contributed equally to this work

Received: 20 September 2005; accepted: 1 March 2006; published online: 6 April 2006

2004). Our data suggested that stalling depends on an interaction between the GAr and a nearby folded domain of the substrate. We hypothesized that the GAr interacts ineffectively with the ATPases of the proteasome; this reduces the efficiency of coupling nucleotide hydrolysis to performing work on the substrate. If the reduction of energy delivery associated with passage of the GAr through the ATPases coincides with a requirement for unfolding, this transient imbalance causes unfolding to fail. Insertion therefore pauses and proteolysis is limited to the portion of the substrate that has already entered the proteolytic chamber. We here describe several independent experimental tests that affirm specific predictions of the model.

Results

Mutations that impair the structural stability of ODC reduce halting

Mouse ornithine decarboxylase (ODC) is a native proteasome substrate with an intrinsic carboxyl-terminal degradation tag (Ghoda *et al*, 1989). Ubiquitin conjugation has no role in ODC degradation (Murakami *et al*, 1992; Coffino, 2001). Its 37-amino-acid carboxyl-terminus (C37) is a portable module sufficient for proteasome recognition and initiation of proteolysis (Ghoda *et al*, 1990). ODC or fusion proteins bearing the ODC C-terminal degradation tag compete with ubiquitin-conjugated proteins and Lys48-linked ubiquitin chains for degradation by the proteasome (Zhang *et al*, 2003). Degradation of ODC is unidirectional and initiates at the degradation tag (Zhang *et al*, 2004). As with almost all proteasome substrates, ODC proteolysis, once initiated, goes to completion. However, inserting a module containing a 30-residue Gly–Ala repeat and short linker sequences (the GAr) after amino acid 424 of mouse ODC, a position just N-terminal to the degradation tag, pauses degradation, producing stable intermediates missing approximately 20, 30 or (more rarely) 45 amino acids from this ODC::GAr_{30} construct (Zhang and Coffino, 2004). ODC truncated after residue 424 (of the full 461 amino-acid protein) has full enzymatic activity, and crystallographic evidence shows that the truncated protein encompasses all parts of the protein that have discernable structure (Kern *et al*, 1999b). Insertion after ODC residue 424 therefore positions the GAr between a well-structured domain and the terminal C37 tag. Crystallographic data reveal a tightly folded β-sheet domain that ends at residue 410, followed immediately by an additional nine residues in a α-helical configuration. The remainder of ODC::GAr_{30} beyond this helix is strongly predicted to lack ordered structure.

We have postulated that ODC::GAr_{30} degradation intermediates accumulate because of an imbalance between the energy delivered by the GAr-impaired proteasome and that needed to unfold the C-terminal β-sheet domain of ODC. By reducing the structural stability of this domain, it should be possible to restore a favorable energy balance during the course of ODC::GAr_{30} degradation. Two outcomes are possible after degradation of a protein substrate begins: complete degradation to peptides or halting. The model we are testing implies that reducing the stability of a structured domain should reduce the probability of the second outcome, resulting in a greater fraction that is fully degraded.

The C-terminus of ODC comprises a β-sheet domain that includes two N-terminal β-strands (B1 and B2, ODC residues 2–19) and one C-terminal B18 β-strand (residues 404–410) (Kern *et al*, 1999b). Upstream of B1 and B2, the N-terminus loops around the B18 β-strand to form a belt-like structure with a short α-helix packed against the C-terminus (see Figure 1A). In this arrangement, the C-terminus of the protein is structurally stabilized by the N-terminus through backbone–backbone contacts in the β-sheet and a series of other interactions, listed in Table I. In order to weaken the C-terminus structure, the N-terminal belt of ODC::GAr_{30} was partially or completely removed by a series of truncations. In addition, a hydrophobic interaction between N- and C-terminal ODC residues was eliminated by replacing Leu14 with Asp (Table I). We sought mutations that would destabilize local structure, but not cause gross misfolding that might divert the protein to other (presumably ubiquitin-dependent) pathways of proteolysis. We expressed these mutant proteins in the yeast *Saccharomyces cerevisiae*, a cellular milieu in which the mechanism of mouse ODC degradation in animal

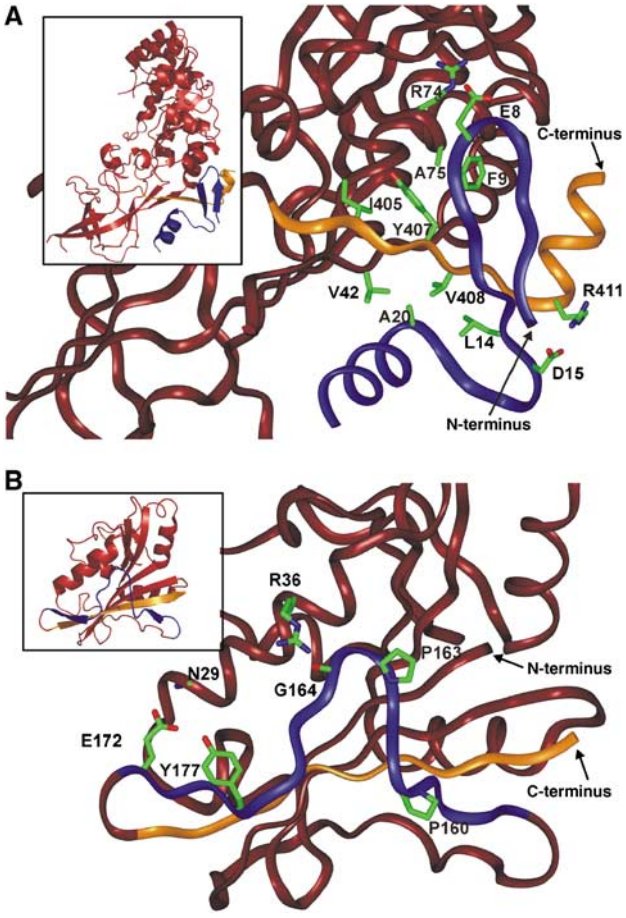

Figure 1 Ribbon diagrams of interactions stabilizing β-sheet domains. (**A**) Mouse ODC (PDB id: 7ODC); inset shows a global view of the monomer. The C-terminus (residues 403–418) is shown in orange and the N-terminus in blue. The side chains of residues involved in stabilizing interactions described in Table I are shown as solid sticks, with carbon atoms in green, oxygen in red and nitrogen in blue. Residues 30–35 are missing from the crystal structure. (**B**) Human DHFR (PDB id: 1DHF); inset shows a global view of the monomer. The C-terminus is shown in orange and the 'safety belt' in blue. Stabilizing residues are shown as solid sticks. For N29 and G164, only the interaction backbone moieties are shown.

Table I Effects of perturbations predicted to alter stability of ODC and DHFR C-terminal β-sheet domains on intermediate accumulation

Altered residue	Relevant mutant	Affected interaction	P_I[a]
None (wild-type ODC)	—	None	1.0
ODC-Glu8	Δ11ODC::GAr_{30}	Glu8-Arg74 (salt bridge)	1.0
ODC-Phe9	Δ11ODC::GAr_{30}	Phe9-Ala75-Tyr407-Ile405 (hydrophobic cluster)	1.0
ODC-Leu14	Δ11ODC^{L14D}::GAr_{30}	Leu14-Ala20-Val42-Val408 (hydrophobic cluster)	0.63
ODC-Asp15	Δ17ODC::GAr_{30}	All of the above, and Asp15-Arg411 (salt bridge)	0.66
None (wild-type DHFR)	—	None	0.31
DHFR-Arg36	DHFR^{R36S}-GAr_{30}-C37	Arg36-Gly164 (polar interaction)	0.36
DHFR-Glu172	DHFR^{E172S}-GAr_{30}-C37	Asn29-Glu172-Tyr177 (polar interaction)	0.10
DHFR-Pro160 and Pro163	DHFR$^{P160A/P163A}$-GAr_{30}-C37	None (form structural loop)	0.07
None (wild-type DHFR)		Methotrexate binding to active site	0.90

[a]The fraction of substrate degradation events that result in stable intermediates (e.g. for $P_I = 1.0$, all degradation events result in intermediates).

cells is conserved (Hoyt *et al*, 2003), and examined their degradation.

As measured by pulse-chase experiments, essentially all the degradation products of ODC::GAr_{30} were intermediates (Figure 2A). At each time point in the chase period, the sum of the intensity of the parent (full-length) protein and the intermediates is approximately constant. Quantitation of the results of three independent pulse-chase experiments of transformants expressing ODC::GAr_{30} (and two informative mutants described below) verified this assessment (Figure 2B). An 11-amino-acid N-terminal truncation (Δ11ODC::GAr_{30}) did not reproducibly alter degradation intermediate accumulation (data not shown). However, the further removal of a stabilizing hydrophobic cluster by the L14D mutation (in Δ11ODC^{L14D}::GAr_{30}) reduced the accumulation of degradation intermediates. With Δ11ODC^{L14D}::GAr_{30}, the sum of the parent and intermediate bands declined during the chase. A significant fraction of processing events therefore resulted in complete degradation (Figure 2A and B). Furthermore, a more extensive truncation of 17 amino acids (Δ17ODC::GAr_{30}) reduced the fraction of products that appeared as intermediates similarly to the Δ11ODC^{L14D}::GAr_{30} fusion protein. In summary, mutations predicted to destabilize the ODC C-terminal β-sheet domain reduced the ability of the GAr element to impede degradation. GAr function thus depends on the stability of the domain proximal to this element. Unfolding has been described as the rate-limiting step in degradation of proteasome substrates (Thrower *et al*, 2000). Consistent with these previous findings, the half-life of ODC::GAr_{30} is about twice that of Δ11ODC^{L14D}::GAr_{30} or Δ17ODC::GAr_{30}, the two mutants bearing the destabilized β-sheet domain (Figure 2B).

The ratio of intermediates can be summarized by the value P_I, the fraction of substrates initiating degradation that end up as intermediates. P_I has a value between zero (no intermediates, parent is completely degraded) and one (only intermediates). This value facilitates comparisons of diverse GAr-containing proteins (Table I). P_I was approximately 1.0 for ODC::GAr_{30}, and was not significantly changed in Δ11ODC::GAr_{30}. However, the further introduction of the L14D mutation in the Δ11ODC^{L14D}::GAr_{30} construct reduced the value of P_I to 0.63. Furthermore, the more extensive truncation of 17 amino acids (Δ17ODC::GAr_{30}) similarly reduced P_I to 0.66.

This analysis requires that the mutations do not stimulate a turnover pathway independent of the ODC degradation signal. To confirm that the proteins were solely degraded in this way, we mutated an essential residue in the degradation tag, corresponding to Cys441 of mouse ODC (Miyazaki *et al*, 1993). A C441A mutation was introduced into the fusion proteins, and in each case prevented degradation (Figure 2C). We conclude that these mutated fusion proteins are degraded by an ODC-specific (and thus proteasome-dependent and ubiquitin-independent) degradation pathway.

Perturbations that alter the structural stability of DHFR also alter halting

Appending the C-terminal degradation signal of ODC to diverse proteins, including dihydrofolate reductase (DHFR), converts them to proteasome substrates (Loetscher *et al*, 1991; Li *et al*, 1998; Zhang *et al*, 2003). To investigate whether the β-sheet domain of DHFR has the potential to interrupt substrate processing by collaborating with a GAr, we constructed a fusion protein containing the entire human DHFR open reading frame followed by the GAr_{30} module and the 37-residue ODC degradation tag, forming DHFR-GAr_{30}-C37.

Pulse-chase analysis showed that DHFR-GAr_{30}-C37 generated a single stable degradation product shorter than the parent molecule (Figure 3A), in which approximately 20 residues were removed from its C-terminus (data not shown). In contrast to ODC::GAr_{30}, which is almost always completely processed to intermediates ($P_I \sim 1.0$), DHFR-GAr_{30}-C37 degradation gave rise to intermediates only about one-third of the time ($P_I \sim 0.3$). Like ODC, the C-terminus of DHFR is a β-strand contained in a β-sheet domain that involves three C-terminal β-strands and one N-terminal β-strand (Prendergast *et al*, 1988). Here, the stability of the C-terminal strand is enhanced by a 'safety-belt' structure, where residues 157–168 loop around the last β-strand. This segment is packed against the strand and anchored to the rest of the molecule through specific interactions (see Figure 1B and Table I). The conformation of this loop is critically dependent on the presence of Pro 160 and Pro 163. To determine whether destabilizing the C-terminal β-sheet domain of the DHFR moiety influenced intermediate accumulation, we followed a strategy similar to that used with ODC. Three mutations anticipated to destabilize the C-terminal β-sheet of DHFR were tested (Figure 1B, Table I). Mutants with a substitution of Arg36 to Ser (DHFR^{R36S}-GAr_{30}-C37), Glu172 to Ser (DHFR^{E172S}-GAr_{30}-C37) or Pro 160 and 163 to Ala (DHFR$^{P160A/P163A}$-GAr_{30}-C37) were constructed and their degradation in yeast cells was examined by pulse-chase analysis. The R36S mutation had little effect on intermediate production and accumulation. However, both the E172S and

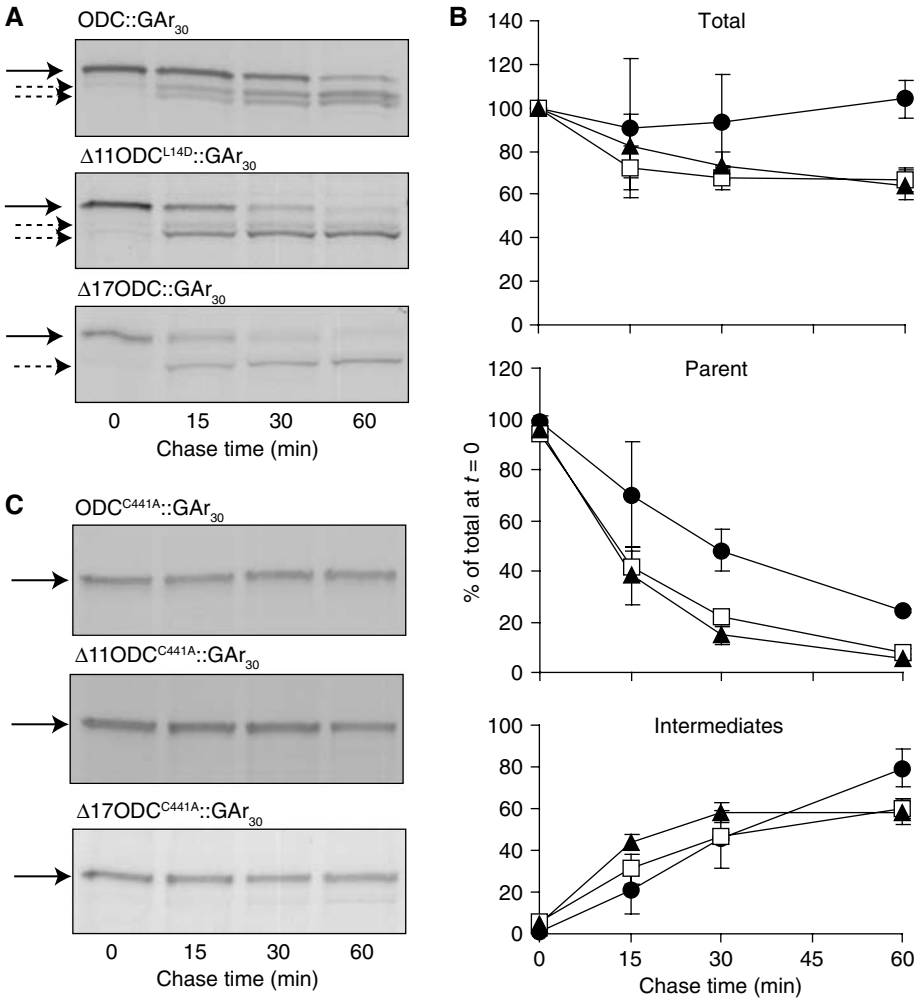

Figure 2 Mutations that disrupt ODC-stabilizing interactions reduce the accumulation of degradation intermediates. (**A**) Pulse-chase analysis of yeast cells expressing wild-type or mutant ODC::GAr_{30} fusion proteins. The position of full-length ODC::GAr_{30} (solid arrow) or degradation intermediates (dashed arrows) is indicated. (**B**) Quantitation of ODC::GAr_{30} turnover data from (A), presented as the mean of three independent experiments. Error bars represent the standard deviation. The values for wild-type ODC::GAr_{30} (●), Δ17ODC::GAr_{30} (□) and $\Delta 11ODC^{L14D}$::GAr_{30} (▲) are expressed as a percentage of the total of the full-length parent fusion protein and its degradation intermediates at time zero. The changes in the wild-type and mutant proteins are compared for the parent molecule (middle panel), its degradation intermediates (bottom panel) and the sum total of these (top panel) at each time point. (**C**) Pulse-chase analysis of ODC::GAr_{30} fusion proteins containing the C441A mutation in the ODC degradation tag. Arrows indicate bands as in (A).

P160A/P163A substitutions had marked effects (Figure 3A). The P_I value for DHFR-GAr_{30}-C37, 0.31, was reduced by the E172S and P160A/P163A mutations, respectively, to 0.10 and 0.07 (Table I). Pulse-chase analysis demonstrated that all three proteins containing a C441A substitution of the critical cysteine were stable (Figure 3B).

Because processing of DHFR-GAr_{30}-C37 is poised to produce either outcome with substantial probability, this construct provides the opportunity to test the consequences of both destabilization and stabilization of the DHFR moiety. Methotrexate binds tightly to the DHFR active site and has been used extensively to impair DHFR unfolding, for example (Eilers and Schatz, 1986). We have previously shown that methotrexate can block degradation of an ODC::DHFR fusion protein (Zhang *et al*, 2004). Yeast cells expressing DHFR-GAr_{30}-C37 were treated with methotrexate or were left untreated and subjected to pulse-chase analysis of turnover and intermediate accumulation (Figure 3C). Treatment with the stabilizing ligand increased P_I three-fold, to 0.90 (Table I). Together, the DHFR-destabilizing mutations and ligand-mediated stabilization provided a bidirectional test of our hypothesis and demonstrated that GAr function is strongly influenced by the stability of an adjacent C-terminal domain.

Position of cutting sites that generate stable intermediates not altered by extending the degradation tag

The model being tested postulates that a structured domain stops insertion of a GAr-containing substrate and thus halts its proteolysis. This implies that the sites at which proteolysis terminates must be positioned by reference to the folded domain, not determined by the configuration of the C-terminal degradation tag. We tested this hypothesis by duplicating the C37 degradation tag of an ODC::GAr_{30} fusion protein, thus adding an additional 38 residues to the C-terminus. We expressed ODC::GAr_{30} fusions with either the normal or extended C-termini in yeast transformants and performed pulse-chase experiments to compare the size of the inter-

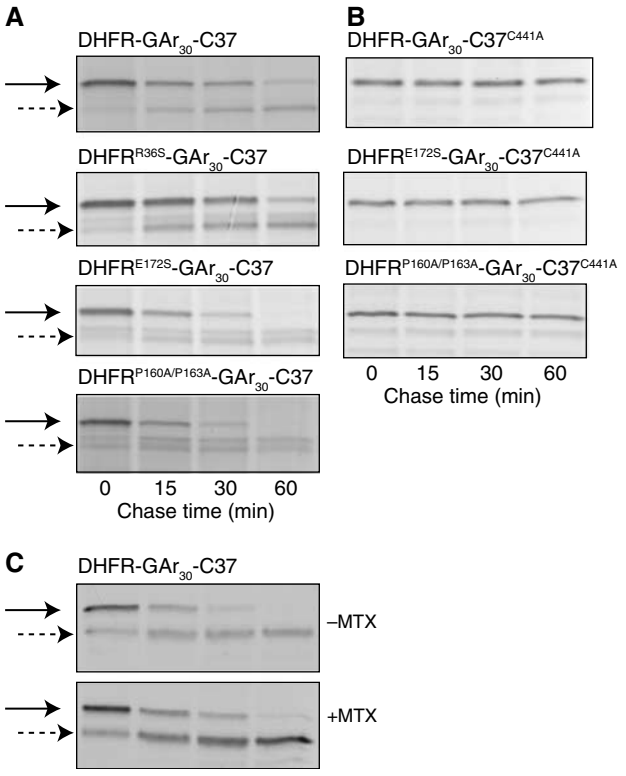

Figure 3 The accumulation of DHFR-GAr_{30}-C37 degradation intermediates is influenced by the stability of the DHFR domain. (**A**) Pulse-chase analysis of wild-type and mutant DHFR-GAr_{30}-C37 proteins. (**B**) Pulse-chase analysis of fusion proteins containing the C441A mutation in the ODC degradation tag. (**C**) Pulse-chase analysis of DHFR-GAr_{30}-C37 in yeast cells either with (+MTX) or without (−MTX) the addition of 20 μM methotrexate. Arrows indicate bands as in Figure 2.

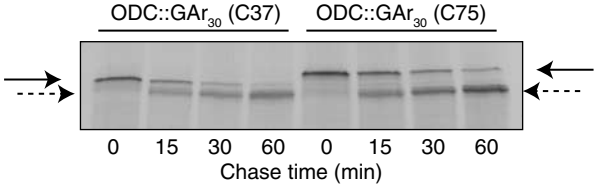

Figure 4 The positions of cutting sites that generate stable intermediates are not altered by extending the degradation tag. Pulse-chase analysis of yeast cells expressing ODC::GAr_{30} fusion proteins with wild-type (C37) or extended (C75) degradation tags. The parent bands and common intermediates are indicated by arrows as in Figure 2.

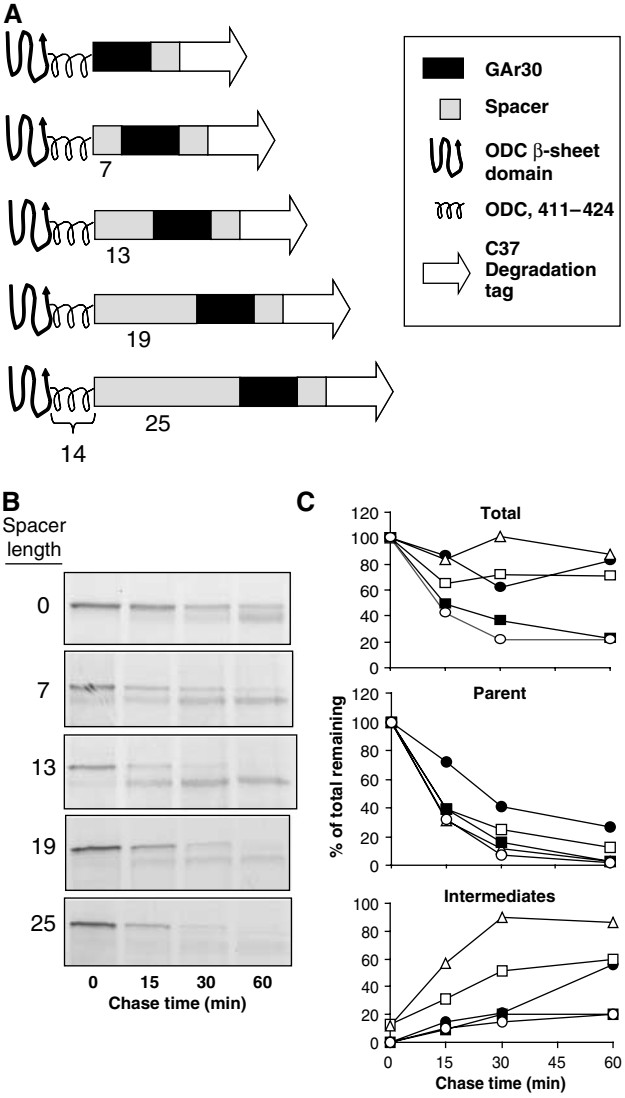

Figure 5 The effects of spacing between GAr and β-sheet domain on production of intermediates. (**A**) Schematic of ODC::GAr_{30} constructs containing spacers of varying length between the ODC C-terminal β-sheet and the GAr_{30} domains. The number of spacer residues is indicated below each construct. (**B**) Pulse-chase analysis of cells expressing constructs in (A). (**C**) Quantitation of turnover data for ODC[n]GAr_{30} fusions in (B) with spacer lengths of 0 (●), 7 (□), 13 (Δ), 19 (■) or 25 (○) residues were analyzed as in Figure 2B.

mediates they produce (Figure 4). As expected, the fractionation of the two full-length fusion proteins by SDS–PAGE was consistent with the expected differences in their molecular mass. The extension of the C-terminus had no apparent effect on the degradation rate of the fusion protein when compared to the unextended molecule. However, the mobility of the intermediates derived from the two proteins during the chase period was not distinguishably different. This implies that cutting is both limited and positioned by structures that lie on the N-terminal side of the sites of terminal proteolysis.

Spacing between GAr and folded domain is critical for halting

Because the functional interaction between the GAr and a folded domain is postulated to require that they arrive simultaneously at their respective sites of action, altering the spacing between these two elements should alter the synchrony of their arrival and thus modify halting. A series of homologous substrates were constructed and expressed in yeast transformants to test this idea (Figure 5A). In the first of these, 0, 7, 13, 19 or 25 residues were inserted between ODC position 424 and the GAr_{30} tract. The constructs with spacer lengths of 0, 7 or 13 residues differed little from ODC::GAr_{30} in the extent of halting (Figure 5B and C); for each of these, most processing events produced intermediates (P_I range 0.68–0.88). However, extending the spacer length to 19 or 25 residues sharply reduced the efficiency of intermediate production ($P_I = 0.21$ and 0.20). Because the folded β-sheet domain of ODC extends to residue 410 (Kern *et al*, 1999a),

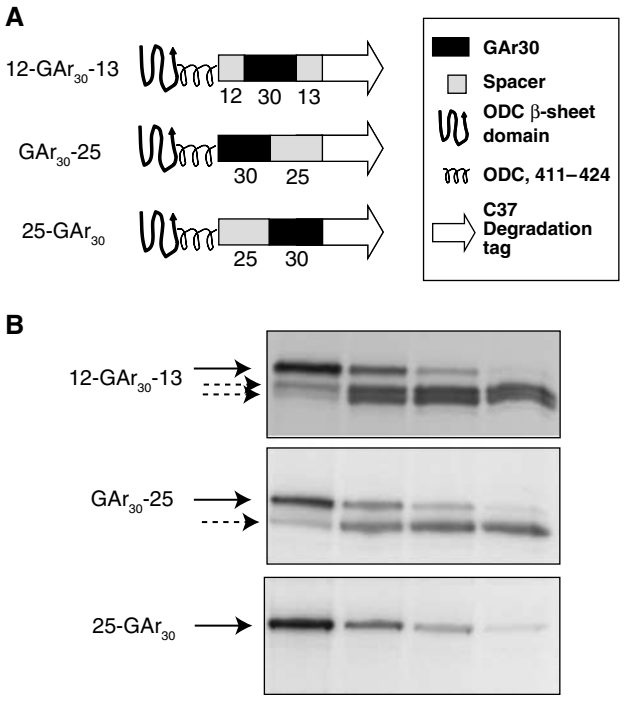

Figure 6 Pulse-chase analysis of ODC::GAr_{30} linker constructs with C-terminal extensions of fixed size. (**A**) Schematic of ODC::GAr_{30} constructs in which the context of the Gly–Ala repeat is varied with respect to its flanking linker sequences. The length of each region in residues is indicated below each construct. (**B**) Pulse-chase analysis of yeast transformants expressing the fusion proteins shown in (A). Arrows indicate bands as in Figure 2.

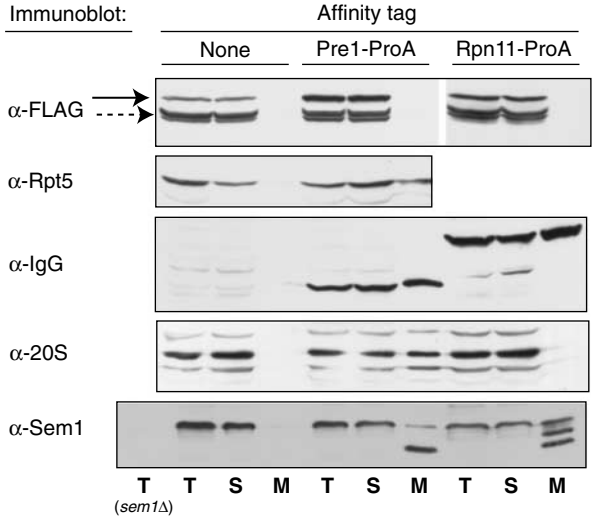

Figure 7 Degradation intermediates do not cofractionate with proteasomes. Lysates were prepared from cells expressing ODC::GAr_{30} and bearing either no proteasome affinity tag or a Protein A (ProA) tag associated with either the Pre1 subunit of the 20S core particle or the Rpn11 subunit of the 19S regulatory complex. Following affinity purification, fractions designated total (T), supernatant (S) and matrix-associated (M) were subjected to SDS–PAGE and immunoblotting; M fractions were overloaded 20-fold compared to the T and S fractions to facilitate visualization of affinity-fractionated, proteasome-associated proteins. Immunoblotting was performed with antibodies specific for the FLAG epitope in the ODC::GAr_{30} substrate (solid arrow) and intermediates (dashed arrow), Rpt5, 20S or Sem1 proteins. ProA-tagged Pre1 and Rpn11 proteasome subunits were detected by the direct interaction of ProA with IgG. Sem1 antibody specificity was confirmed using extracts from a *sem1*Δ strain as negative control; the additional Sem1-specific bands of lower apparent molecular weight cofractionating with the proteasome were not further characterized.

14 residues lie between the end of the β-sheet domain and ODC residue 424. Therefore, the presence of 33 or 39 residues between the β-sheet domain and the GAr_{30} tract reduced its function, whereas 27 or fewer did not. (As reference, in ODC::GAr_{30} used in the experiments described above, the β-sheet domain-GAr distance is 26 residues.)

In the above series of constructs, all structural elements were held constant except for the distance between the β-sheet domain and the GAr_{30}. Consequently, the distance between ODC residue 424 and the C37 degradation tag, which in the native protein immediately follows position 424, ranged from 30 to 55 residues. To determine whether this variable rather than the distance between the β-sheet domain and the GAr is the critical parameter determining intermediate production, we compared three constructs in which the spacing between ODC position 424 and C37 (Figure 6) was identical. Moving all 25 flanking residues to the GAr C-terminal side produced abundant intermediates, similar to the standard ODC::GAr_{30} fusion protein. In contrast, when the 25 residue flanking sequence was placed on the N-terminal side of the GAr, no intermediates were detected. This result supports the inference from the experiments above that the critical variable is the spacing between the β-sheet domain and the GAr_{30}.

Intermediates are not trapped by proteasome

For the substrates described here to undergo partial proteolysis, a part of their C-terminal end must have reached the proteolytic chamber of the proteasome 20S core particle, while a folded region of the same protein remains positioned elsewhere, likely within or contiguous to the 19S regulatory complex. We asked whether, when insertion ceases, the substrate remains in an inserted mode, persistently associated with the proteasome, or escapes instead. To address these questions, we expressed ODC::GAr_{30} in a yeast strain in which proteasomes had been equipped with an affinity tag to facilitate their rapid isolation. Proteasomes were fractionated from substrates and their degradation intermediates in buffer containing ATP. We first affinity purified proteasomes with a protein A tag fused to the β4 (Pre1) subunit of the 20S proteolytic core. Western blotting for 20S proteins and for the 19S component Rpt5 demonstrated that both 20S and 19S complexes were recovered with similar efficiencies in the matrix-bound fraction—absolute recoveries were 5–10% (Figure 7). This shows that the buffer composition and fractionation conditions used effectively maintained an association between the 20S core and 19S regulatory complex. Neither 20S proteins nor Rpt5 were associated with the affinity matrix in a control strain lacking the affinity tag. To increase the sensitivity of detection for trapped intermediates, a 20-fold excess of the affinity pulldown fractions was analyzed compared to total and supernatant fractions.

We observed no intermediates of degradation (nor parent substrate) associated with the proteasomes bound to the affinity matrix via the Pre1 tag (Figure 7, Pre1-ProA tag). ODC::GAr_{30} or its processed intermediates were visualized only in the total cell lysate or in the supernatant fraction

following the pulldown or in the control nontagged pulldown. We also performed similar experiments using a protein A tag fused to the Rpn11 (Figure 7, Rpn11-ProA tag) or Rpn1 (data not shown) subunits of the 19S complex, with similar results. Sem1 is a protein that has been recently identified as a component of the proteasome 19S complex (Funakoshi *et al*, 2004; Sone *et al*, 2004). However, the bulk of Sem1 is found in low molecular weight fractions (Funakoshi *et al*, 2004), and recombinant Sem1 readily becomes incorporated into proteasomes from Sem1-deficient cells (Sone *et al*, 2004). These properties suggest Sem1 exists in exchangeable free and proteasome-bound pools. We therefore tested Sem1 recovery as a positive control for proteasome association, using the identical pulldown and processing conditions that are used for ODC::GAr_{30}. Sem1, in contrast to ODC::GAr_{30} and its derivatives, was readily visualized in pulldown fractions from Pre1- or Rpn11-ProA-tagged strains. We conclude, therefore, that ODC::GAr_{30} intermediates are not persistently trapped in the 20S proteasome. Gel filtration fractionation of ODC::GAr_{30} and its intermediates from untagged proteasomes supported the same conclusion (data not shown). Together, these results exclude persistent intermediate trapping by 19S, 20S or 26S forms of the proteasome. We also performed the converse experiment, using an internal FLAG epitope tag within ODC::GAr_{30} to perform the pulldown and Western blots to evaluate the recovery of proteasome proteins in association with ODC::GAr_{30} or its derivatives. None were detected (data not shown).

Complete degradation of a mouse ODC molecule expressed in *S. cerevisiae* takes about 10 min (Hoyt *et al*, 2003). In the pulldown experiments, approximately 45 min elapsed between cell lysis and completion of fractionation. We therefore cannot infer whether exit takes place at a rate comparable to the normal process of complete degradation or is more rapid.

Discussion

We have previously proposed (Zhang and Coffino, 2004), and here test, the following simple model: Two elements of the 19S regulatory particle are postulated to function coordinately. The first is a site impelling translocation, the ATPase ring, which binds the substrate and advances it stepwise toward the 20S core particle. The second is a site of constriction within the regulatory particle, possibly the entrance to a translocation channel through the ATPase ring. This postulated constriction impairs transit of a folded domain. The ATPase ring produces energy that performs work on the substrate, some of which is used to unravel the folded domain. The mode of energy transmission may be as simple as a lever arm motion that applies a friction drive to the polypeptide chain (Hinnerwisch *et al*, 2005). In the normal case, energy supply continuously exceeds need, and the substrate polypeptide continuously advances. If this balance transiently swings in the other direction, with energy need exceeding supply, insertion halts. If the substrate has penetrated sufficiently far into the core particle, proteolysis is limited by the failure to advance further. The position at which the substrate is cut reflects the furthest extent of penetration into the proteolytic chamber. The remaining substrate is released, and, if proteolysis has removed the degradation tag, partial proteolytic products persist as stable degradation intermediates.

Insertion can be stopped by a modestly stable folded structure if the capacity of the ATPase ring to transmit energy becomes impaired. The arrival of a GAr at the ATPase site is postulated to produce such impairment. This may happen because the tract of glycines and alanines (the two smallest amino acids) presents a relatively featureless face to an ATPase-associated friction drive apparatus that normally advances the chain. This conjecture is consistent with the known substrate interaction properties of bacterial ATPases. ClpB, in collaboration with the DnaK chaperone system, solubilizes and refolds aggregated proteins. Its binding site (near the axial pore of the ATPase hexamer) prefers substrates with aromatic and basic residues (Schlieker *et al*, 2004). The HslU ATPase of the HslUV bacterial protease has a similar preference for aromatic and positively charged amino acids at substrate residue positions important for recognition (Burton *et al*, 2005).

Here, we tested this model in several ways. First, we altered the stability of an ODC or DHFR folded domain by introducing mutations expected to cause destabilization or (for DHFR) by adding a stabilizing ligand. Within ODC::GAr_{30}, deletions were designed to destroy interactions that stabilize the β-sheet domain proximal to the GAr and the C37 degradation tag. Using DHFR constructs, we pursued a similar strategy and obtained a similar result: mutations directed toward reducing stability reduced intermediate production. DHFR also provided the opportunity to examine the effect of domain stabilization on intermediate production. The stabilizing ligand methotrexate markedly increased the appearance of intermediates. These findings are consistent with a model of protease function described by Matouschek and co-workers (Lee *et al*, 2001; Prakash *et al*, 2004) who showed that the proteasome unfolds and degrades substrates sequentially from an unstructured initiation site.

Alternative mechanisms through which a GAr might produce degradation intermediates are less tenable. A GAr may enhance endoproteolytic cleavage by the proteasome (Liu *et al*, 2002a) and thus leave the remainder of the GAr-containing fusion protein unprocessed. Such a model seems unlikely, however, given that GAr function depends on the stability of structural domains spatially distinct from the GAr itself. Our data also exclude mechanisms whereby substrate processing initiates, but ceases when components of the proteasome encounter a GAr and become immobilized. Such a sabotage mechanism implies the stable association of intermediate with proteasome, contrary to our data showing that their association is transient.

In addition to the anticipated quantitative effect of changing domain stability, an unanticipated change in the pattern of intermediates was also seen. ODC::GAr_{30} produces three intermediates, missing about 20, 30 and (more rarely) 45 residues from its C-terminus. This suggests that the insertion process overcomes a series of energy barriers, a process in which progressive clipping marks progressive subdomain unfolding events. The mutations we have investigated uniformly reduced the accumulation of the intermediate missing ~20 residues, but had little effect on the others (Figure 2A). This is consistent with selective reduction of the most proximal energy barrier, while more distal ones are little disturbed, a result that might have been expected from the strategy of mutant design.

In a further independent test of the model, we varied the spacing between the folded domain of ODC (assumed here to end at the terminal β18 strand (Kern *et al*, 1999a)) and the proximal boundary of a GAr of length 30. A distance of 14, 21 or 27 amino acids between these elements led to efficient stalling of insertion. Increasing this distance to 33 amino acids strongly reduced stalling and an increase to 39 further reduced it. The distance between successive α-carbon atoms of an extended polypeptide chain is ~3 Å, and so these spacings of 14, 21 or 27 residues are equivalent to about 40, 60 and 80 Å. Our data imply that the minimum separation that supports functional interaction is 40 Å or less. The result is consistent with the possibility that the two functional sites in fact colocalize. This is credible: if the substrate threads through an axial pore of an ATPase annulus, the pore could be the site of restriction. Separating the two elements by 100 Å (33 residues) or more strongly impairs their capacity to collaborate. The full 19S regulatory complex seen by electron microscopy can be encompassed within a sphere about 150 Å in diameter (Walz *et al*, 1998). Failure of interaction at distances approaching the dimensions of the 19S complex is consistent with the requirement that both sites lie within the complex.

By using pulse-chase data, we calculated the fraction of processed substrates that partition to intermediates, P_I, and used this as the primary analytic tool for examining halting of proteolysis. P_I has a simple physical interpretation: it corresponds to the probability that degradation, once initiated, will cease. This can also be expressed as a ratio of rate constants, whereby a substrate that is undergoing degradation will alternatively undergo further degradation at a rate k_D or stop degradation (and likely exit the proteasome) at a rate k_I. Then, $P_I = k_I/(k_I + k_D)$. The proteasome is generally assumed to operate on most ordinary substrates with a P_I that is close to zero. This is based on the perception that degradation appears to be completed once it is begun. The conclusion, however, rests largely on our failure to observe intermediates. Two considerations limit our capacity for detecting the presence or production of intermediates. The first of these is technical: SDS–PAGE, the most commonly used means to follow proteolysis, readily detects abundant protein species of discrete size, but not lower abundance populations of heterogeneous size. Therefore, only intermediates consisting of discrete molecular species, like those described here, will be observed readily. Second, degradation intermediates may include misfolded elements; these proteins may be subjected to a second round of elimination by the ubiquitin–proteasome system, thereby escaping detection. The value of P_I for typical substrates therefore remains an open question.

Understanding the import machinery of the proteasome can benefit from considering better-understood models of protein translocation, such as membrane transport systems or bacterial ATP-dependent proteases. In principle, two mechanisms can be utilized, either a power stroke or Brownian ratchet. By analogy with other systems in which ATPases are used (Singleton *et al*, 2000; Kenniston *et al*, 2003; DeLaBarre and Brunger, 2005; Hinnerwisch *et al*, 2005), a power stroke model is the more likely. Consideration of the power stroke mechanism may help to illuminate why the native GAr is so long: a long GAr assures probabilistic iterative failure. If the bacterial ClpXP protease is presented with a multidomain substrate, it releases the substrate at an appreciable frequency, yielding stable intermediates that are cut between domain boundaries. A titin domain interrupts processing by ClpXP about one time in three (Kenniston *et al*, 2005). This significant failure rate ($P_I \sim 0.3$) does not require mediation by a recognizable GAr-like sequence. The proteasome may be a more powerful machine, so that a folded domain must be supplemented by a slippery sequence to cause a comparable rate of failure. Alternatively, the titin domain may have more stringent unfolding requirements than those we have tested in the proteasome. As discussed above, it is also possible that proteasomes have a P_I that significantly exceeds zero for native folded proteins.

The Epstein–Barr virus has evolved a tract of 60–300 residues (in different isolates), which are exclusively glycines and alanines. A sequence of such length did not likely evolve to confer a global folding property, nor is it easy to imagine a specific proteasome site that requires for interaction (or impairment of interaction) the full span of a sequence of such length and invariant composition. Much more likely is a requirement for iterative impairment of many such interactions, performed as the polypeptide chain advances through the proteasome. Each completed power stroke thrust would, in this view, displace the next such interaction to a new position along the chain, a displacement equal to the power stroke length. The estimated power stroke length of other AAA ATPase motors, such as bacteriophage T7 helicase, is about 20 Å (Singleton *et al*, 2000), which corresponds to an extended peptide of about seven residues. Suppose that failure of a single iteration of displacement causes substrate release. A GAr of 300 residues would suffer that risk more than 40 times, converting, for example, a 90% success rate per iteration to a success rate of 1% for traversing the full sequence ($P_I \sim 0.99$). When suitably juxtaposed to a folded ODC domain, a GAr as short as seven residues can cause failure of processive degradation about one time in three ($P_I \sim 0.3$). A long GAr would require neither exquisite positioning nor unidirectional chain processing, and would assure that processivity is interrupted, even when the failure rate per individual iteration is low.

Our data support the conclusion that degradation intermediates are released from the proteasome, a finding also true of ClpXP (Kenniston *et al*, 2005). Intermediate release has several implications. First, it assures that the proteasome system will not be functionally depleted by persistent futile interactions. Second, it is consistent with a few exceptional cases in which proteasomes are used for processing rather than complete degradation (Rape and Jentsch, 2002). Converting certain precursor proteins to mature transcription factors requires them to be partially proteolyzed by proteasomes and then liberated. One such transcription factor is NFκB, the p50 subunit of which is generated from a p105 precursor by proteasomal truncation of its C-terminal end. It is of interest that producing the p50 intermediate requires both a structured domain within the N-terminal end of the p105 precursor and a glycine-rich tract near the processing junction. Removing the glycine-rich region (Orian *et al*, 1999) or impairing the stability of the folded domain (Lee *et al*, 2001) or increasing spacing between the two (Tian *et al*, 2005) reduces halting, biasing degradation toward completion rather than production of the p50 protein. Although the functional interactions of these elements obviously resemble

those within the more artificial substrates we have studied, it remains to be determined whether the glycine-rich region of the p105 precursor confers functional properties similar to a GAr.

Materials and methods

Yeast strains

All GAr-containing fusion proteins were expressed from p414ADH-based vectors (Mumberg *et al*, 1995) in *S. cerevisiae* strain MHY501 (*MAT*α *his3-*Δ*200 leu2-3,112lys2-801 trp1-1 ura3-52*) (Chen *et al*, 2002), unless otherwise noted. All yeast strains were maintained and manipulated using standard procedures (Guthrie and Fink, 1991). Strains MHY85 and MHY94, bearing C-terminal *Staphylococcus aureus* protein A tags on proteasome subunits Pre1 and Rpn11, respectively, were generated by the integration of the tag sequence and the *Kluyveromyces lactis TRP1* gene at their chromosomal loci in strain MHY501 using described methods (Knop *et al*, 1999). For this transformation, a DNA fragment encoding the TEV protease cleavage site, two protein A IgG-binding domains, and the *K. lactis* TRP1 gene, and flanked by 50 bp *PRE1* or *RPN11* chromosomal sequences to direct integration, was amplified from the TAP tag vector pBS1479 (Puig *et al*, 2001) by PCR.

Plasmid construction

Details of the construction of plasmids used in this study are provided in supplementary data.

Metabolic labeling, immunoprecipitations and substrate-trapping assay

Pulse-chase analysis was performed as described previously (Hoyt *et al*, 2003). GAr_{30}-containing fusion proteins were immunoprecipitated using FLAG epitope tags located either within the GAr_{30} module itself, or at the N-terminus of the fusion protein, using anti-FLAG M2 affinity gel (Sigma).

Yeast strains bearing a Protein A affinity tag appended to the C-terminus of the Pre1 (strain MHY85) or Rpn11 (MHY94) proteasome subunits were transformed with a *URA3*-marked low-copy vector (p416ADH, (Mumberg *et al*, 1995)) expressing ODC::GAr_{30} (pJ67). Strain MHY501 was used as a negative control. For cofractionation experiments, 40 ml cultures of the transformants were harvested in late exponential growth phase ($OD_{600} = \sim 1.5$), washed with water, and resuspended in 300 μl lysis buffer (50 mM Tris–HCl pH 7.5, 150 mM NaCl, 10% glycerol, 2 mM ATP and 5 mM $MgCl_2$). The cells were mechanically disrupted in 2-ml screw-top microcentrifuge tubes with 200 μl glass beads in a Mini-beadbeater (Biospec Products) for four pulses of 30 s duration with 30 s cooling on ice between pulses. The lysates were cleared by centrifugation (18 000 *g*, 15 min) and 750 μg of total protein in 0.5 ml total volume was incubated with 5 μl of either rabbit IgG agarose or anti-Flag M2 agarose at 4°C for 20 min. The affinity-purified proteasome complexes were washed four times with 500 μl lysis buffer, resuspended in Laemmli SDS–PAGE loading buffer, and fractionated by SDS–PAGE. The fractioned proteins were transferred to nitrocellulose filters, and the filters were blocked in Tris-buffered saline with 1% Triton X-100 (TBS-T) including 5% powdered low-fat milk, and rinsed briefly with TBS-T. Proteins were detected with mouse anti-FLAG M2 antibody (Sigma, 1:2000 dilution) and TrueBlot anti-mouse Ig-horseradish peroxidase conjugates (eBioscience, 1:4000), or rabbit anti-Rpt5 (BioMol, 1:25000), anti-20S proteasome antibodies (gift of T Tamura, 1:2000) or anti-yeast Sem1 antibodies (gift of M Funakoshi, 1:5000) and TrueBlot anti-rabbit Ig-horseradish peroxidase conjugates (1:4000). Immunoblots were developed using the Amersham ECLplus detection kit and protocol.

Data quantification

Signals from autoradiographic films were quantified using TotalLab software (Nonlinear Dynamics). Data for the calculation of P_I (see Discussion) was obtained from pulse-chase experiments with 60 min chase periods. The term k_I was calculated as the accumulation of intermediates between 0 and 60 min (Int_{60}–Int_0) divided by the parent molecules lost during the same interval (P_0–P_{60}). Similarly, the term k_D was calculated as $(P_0–P_{60}) + (Int_0–Int_{60})/(P_0 + Int_0)$. $P_I = k_I/(k_I + k_D)$.

Supplementary data

Supplementary data are available at *The EMBO Journal* Online.

Acknowledgements

We thank Tomohiro Tamura, Daniel Finley, Kiran Madura and Minoru Funakoshi for reagents, and Fred Cohen and George Oster for helpful comments on the manuscript. This work was supported by NIH grants GM45335 and GM074760 to PC.

References

Burton RE, Baker TA, Sauer RT (2005) Nucleotide-dependent substrate recognition by the AAA+ HslUV protease. *Nat Struct Mol Biol* **12:** 245–251

Chen H, MacDonald A, Coffino P (2002) Structural elements of antizymes 1 and 2 required for proteasomal degradation of ornithine decarboxylase. *J Biol Chem* **277:** 45957–45961

Coffino P (2001) Regulation of cellular polyamines by antizyme. *Nat Rev Mol Cell Biol* **2:** 188–194

DeLaBarre B, Brunger AT (2005) Nucleotide dependent motion and mechanism of action of p97/VCP. *J Mol Biol* **347:** 437–452

Eilers M, Schatz G (1986) Binding of a specific ligand inhibits import of a purified precursor protein into mitochondria. *Nature* **322:** 228–232

Funakoshi M, Li X, Velichutina I, Hochstrasser M, Kobayashi H (2004) Sem1, the yeast ortholog of a human BRCA2-binding protein, is a component of the proteasome regulatory particle that enhances proteasome stability. *J Cell Sci* **117:** 6447–6454

Ghoda L, Phillips MA, Bass KE, Wang CC, Coffino P (1990) Trypanosome ornithine decarboxylase is stable because it lacks sequences found in the carboxyl terminus of the mouse enzyme which target the latter for intracellular degradation. *J Biol Chem* **265:** 11823–11826

Ghoda L, van Daalen Wetters T, Macrae M, Ascherman D, Coffino P (1989) Prevention of rapid intracellular degradation of ODC by a carboxyl-terminal truncation. *Science* **243:** 1493–1495

Glickman MH, Rubin DM, Fried VA, Finley D (1998) The regulatory particle of the *Saccharomyces cerevisiae* proteasome. *Mol Cell Biol* **18:** 3149–3162

Groll M, Ditzel L, Lowe J, Stock D, Bochtler M, Bartunik HD, Huber R (1997) Structure of 20S proteasome from yeast at 2.4A resolution. *Nature* **386:** 463–471

Guthrie C, Fink GR (eds) (1991) *Guide to Yeast Genetics and Molecular Biology*. San Diego: Academic Press

Hinnerwisch J, Fenton WA, Furtak KJ, Farr GW, Horwich AL (2005) Loops in the central channel of ClpA chaperone mediate Protein binding, unfolding, and translocation. *Cell* **121:** 1029–1041

Hoyt MA, Zhang M, Coffino P (2003) Ubiquitin-independent mechanisms of mouse ornithine decarboxylase degradation are conserved between mammalian and fungal cells. *J Biol Chem* **278:** 12135–12143

Kenniston JA, Baker TA, Fernandez JM, Sauer RT (2003) Linkage between ATP consumption and mechanical unfolding during the protein processing reactions of an AAA+ degradation machine. *Cell* **114:** 511–520

Kenniston JA, Baker TA, Sauer RT (2005) Partitioning between unfolding and release of native domains during ClpXP degradation determines substrate selectivity and partial processing. *Proc Natl Acad Sci USA* **102:** 1390–1395

Kern AD, Oliveira MA, Coffino P, Hackert ML (1999a) Structure of mammalian ornithine decarboxylase at 1.6 # resolution: stereochemical implications of PLP-dependent amino acid decarboxylases. *Structure* **7:** 567–581

Kern AD, Oliveira MA, Coffino P, Hackert ML (1999b) Structure of mammalian ornithine decarboxylase at 1.6 A resolution: stereochemical implications of PLP-dependent amino acid decarboxylases. *Struct Fold Des* **7:** 567–581

Knop M, Siegers K, Pereira G, Zachariae W, Winsor B, Nasmyth K, Schiebel E (1999) Epitope tagging of yeast genes using a PCR-based strategy: more tags and improved practical routines. *Yeast* **15:** 963–972

Lee C, Schwartz MP, Prakash S, Iwakura M, Matouschek A (2001) ATP-dependent proteases degrade their substrates by processively unraveling them from the degradation signal. *Mol Cell* **7:** 627–637

Levitskaya J, Coram M, Levitsky V, Imreh S, Steigerwald-Mullen PM, Klein G, Kurilla MG, Masucci MG (1995) Inhibition of antigen processing by the internal repeat region of the Epstein–Barr virus nuclear antigen-1. *Nature* **375:** 685–688

Levitskaya J, Sharipo A, Leonchiks A, Ciechanover A, Masucci MG (1997) Inhibition of ubiquitin/proteasome-dependent protein degradation by the Gly-Ala repeat domain of the Epstein–Barr virus nuclear antigen 1. *Proc Natl Acad Sci USA* **94:** 12616–12621

Li X, Zhao X, Fang Y, Jiang X, Duong T, Fan C, Huang CC, Kain SR (1998) Generation of destabilized green fluorescent protein as a transcription reporter. *J Biol Chem* **273:** 34970–34975

Liu CW, Corboy MJ, DeMartino GN, Thomas PJ (2002a) Endoproteolytic activity of the proteasome. *Science* **12:** 12

Liu CW, Millen L, Roman TB, Xiong H, Gilbert HF, Noiva R, DeMartino GN, Thomas PJ (2002b) Conformational remodeling of proteasomal substrates by PA700, the 19 S regulatory complex of the 26 S proteasome. *J Biol Chem* **277:** 26815–26820

Loetscher P, Pratt G, Rechsteiner M (1991) The C terminus of mouse ornithine decarboxylase confers rapid degradation on dihydrofolate reductase. *J Biol Chem* **266:** 11213–11220

Lowe J, Stock D, Jap B, Zwickl P, Baumeister W, Huber R (1995) Crystal structure of the 20S proteasome from the archaeon T. acidophilum at 3.4 A resolution. *Science* **268:** 533–539

Miyazaki Y, Matsufuji S, Murakami Y, Hayashi S (1993) Single amino-acid replacement is responsible for the stabilization of ornithine decarboxylase in HMOA cells. *Eur J Biochem* **214:** 837–844

Mumberg D, Muller R, Funk M (1995) Yeast vectors for the controlled expression of heterologous proteins in different genetic backgrounds. *Gene* **156:** 119–122

Murakami Y, Matsufuji S, Kameji T, Hayashi S, Igarashi K, Tamura T, Tanaka K, Ichihara A (1992) Ornithine decarboxylase is degraded by the 26S proteasome without ubiquitination. *Nature* **360:** 597–599

Orian A, Schwartz AL, Israel A, Whiteside S, Kahana C, Ciechanover A (1999) Structural motifs involved in ubiquitin-mediated processing of the NF-kappaB precursor p105: roles of the glycine-rich region and a downstream ubiquitination domain [In Process Citation]. *Mol Cell Biol* **19:** 3664–3673

Pickart CM, Cohen RE (2004) Proteasomes and their kin: proteases in the machine age. *Nat Rev Mol Cell Biol* **5:** 177–187

Prakash S, Tian L, Ratliff KS, Lehotzky RE, Matouschek A (2004) An unstructured initiation site is required for efficient proteasome-mediated degradation. *Nat Struct Mol Biol* **11:** 830–837

Prendergast NJ, Delcamp TJ, Smith PL, Freisheim JH (1988) Expression and site-directed mutagenesis of human dihydrofolate reductase. *Biochemistry* **27:** 3664–3671

Puig O, Caspary F, Rigaut G, Rutz B, Bouveret E, Bragado-Nilsson E, Wilm M, Seraphin B (2001) The tandem affinity purification (TAP) method: a general procedure of protein complex purification. *Methods* **24:** 218–229

Rape M, Jentsch S (2002) Taking a bite: proteasomal protein processing. *Nat Cell Biol* **4:** E113–E116

Rubin DM, Glickman MH, Larsen CN, Dhruvakumar S, Finley D (1998) Active site mutants in the six regulatory particle ATPases reveal multiple roles for ATP in the proteasome. *EMBO J* **17:** 4909–4919

Schlieker C, Weibezahn J, Patzelt H, Tessarz P, Strub C, Zeth K, Erbse A, Schneider-Mergener J, Chin JW, Schultz PG, Bukau B, Mogk A (2004) Substrate recognition by the AAA+ chaperone ClpB. *Nat Struct Mol Biol* **11:** 607–615

Singleton MR, Sawaya MR, Ellenberger T, Wigley DB (2000) Crystal structure of T7 gene 4 ring helicase indicates a mechanism for sequential hydrolysis of nucleotides. *Cell* **101:** 589–600

Sone T, Saeki Y, Toh-e A, Yokosawa H (2004) Sem1p is a novel subunit of the 26 S proteasome from *Saccharomyces cerevisiae*. *J Biol Chem* **279:** 28807–28816

Thrower JS, Hoffman L, Rechsteiner M, Pickart CM (2000) Recognition of the polyubiquitin proteolytic signal. *EMBO J* **19:** 94–102

Tian L, Holmgren RA, Matouschek A (2005) A conserved processing mechanism regulates the activity of transcription factors Cubitus interruptus and NF-kappaB. *Nat Struct Mol Biol* **12:** 1045–1053

Vale RD (2000) AAA proteins. Lords of the ring. *J Cell Biol* **150:** F13–F19

Walz J, Erdmann A, Kania M, Typke D, Koster AJ, Baumeister W (1998) 26S proteasome structure revealed by three-dimensional electron microscopy. *J Struct Biol* **121:** 19–29

Zhang M, Coffino P (2004) Repeat sequence of Epstein–Barr Virus EBNA1 protein interrupts proteasome substrate processing. *J Biol Chem* **279:** 8635–8641

Zhang M, MacDonald AI, Hoyt MA, Coffino P (2004) Proteasomes begin ornithine decarboxylase digestion at the carboxy terminus. *J Biol Chem* **279:** 20959–20965

Zhang M, Pickart CM, Coffino P (2003) Determinants of proteasome recognition of ornithine decarboxylase, a ubiquitin-independent substrate. *EMBO J* **22:** 1488–1496